# Androgen Responsive Clusterin Expression in the Developing and Regenerating Mouse Prostate

by Natalie Orsi

B.A. in Biochemistry, May 2014, Augustana College

A Thesis submitted to

The Faculty of
The Columbian College of Arts and Sciences
of the George Washington University
in partial fulfillment of the requirements
for the degree of Master of Science

May 17, 2020

Thesis directed by

Maho Shibata
Assistant Professor of Anatomy and Cell Biology

© Copyright 2020 by Nataile Orsi
All rights reserved

## Dedication

Firstly, I wish to dedicate this thesis to my family. Without their support and encouragement, I would not have moved across the country in pursuit of this degree. I would especially like to thank my mother for being an excellent example of a woman who works hard to achieve success both in academics and in life.

I would also like to dedicate this thesis to my fiancé, who has been my biggest cheerleader. Your love and support over the past two years has kept me calm and grounded, even in stressful times.

Last but certainly not least, I would like to dedicate this thesis to Dr. Maho Shibata, whose guidance and mentorship have been invaluable in this process. She and the other members of the Shibata lab have been a constant source of guidance, encouragement, and help.

**Acknowledgements**

I wish to acknowledge Hunain Khawaja, Andrew Pletcher, Ashutosh Yende, and Tejashree Joglekar as individuals who have been wonderful lab colleagues. Each of them has helped me throughout this project and I am so grateful for their support.

**Abstract of Thesis**

Androgen Responsive Clusterin Expression in the Developing and Regenerating Mouse Prostate

Androgen deprivation is an effective first line of treatment for prostate cancer, yet new approaches for treatment are needed, as many prostate cancers will ultimately develop resistance. Because much of prostate organogenesis occurs when androgen levels are low, we hypothesized that both androgen receptor (AR)-dependent and AR-independent progenitor cells may exist in the developing prostate. To understand the heterogeneity of prostate epithelial cells at a molecular level, we analyzed single cell RNA sequencing (scRNA-seq) data from developing mouse prostates at postnatal day 0, week(s) -1, -4, -6, and adult prostates at 10 weeks. At each of these timepoints, we identified a population of luminal epithelial cells that expressed *Clusterin*, which encodes a chaperone protein that has previously been implicated in prostate cancer and is reported to have anti-apoptotic effects.

Because Clusterin is expressed in cells responsible for intestinal epithelial regeneration following injury, we assessed whether Clusterin may also have similar functions during androgen-mediated regeneration in the mouse prostate. Mice were castrated to induce prostate regression and then implanted with testosterone pumps. We assessed Clusterin expression during prostate regeneration by conducting immunofluorescence (IF) staining. We also assessed AR expression in Clusterin-expressing cells by conducting co-staining using antibodies for Clusterin and AR. In developing prostates from 4-week-old mice and in regenerating prostates, we detected

Clusterin expression in a small number of luminal cells, many of which expressed high levels of AR, and were enriched at the tips of prostate tufts. The number of Clusterin-expressing cells increased as regeneration progressed, suggesting a response to hormones in these cells.

Our findings suggest that Clusterin is a marker for AR-responsive progenitor cells in the normal prostate, and are consistent with previous research that has shown that AR is a transcriptional activator of *Clusterin*. These findings warrant further studies on the inhibition of Clusterin as a treatment for castration-resistant prostate cancers that continue to be dependent on AR signaling.

## Table of Contents

**Dedication**……...……...…iii

**Acknowledgements**……..…….....iv

**Abstract of Thesis**……..……v

**List of Figures**……..……...viii

**List of Tables**……...……..ix

**List of Symbols/Nomenclature**……..……x

Chapter 1: Introduction……1

Chapter 2: Methods……..8

Chapter 3: Results……..12

Chapter 4: Discussion……24

References……..29

## List of Figures

Figure 1: Anatomy of Human and Mouse Prostate…….3

Figure 2: scRNA-seq data highlighting *Clu* expression…….13

Figure 3: *Clu* expression at 4W compared to proximal, basal, luminal, and proliferative markers…….....15

Figure 4: Immunofluorescent staining for Clu in neonatal, prepubescent, and pubescent mice.……..16

Figure 5: Clu expression in regressed and regenerated prostates …….18

Figure 6: Clu expression in the proximal and distal prostate ……20

Figure 7: Immunofluorescence co-staining for Clu and Ki-67 proliferation marker ……21

Figure 8: Immunofluorescence staining of luminal organoids grown in 3D culture conditions……...23

## List of Tables

Table 1: Information of antibodies used for immunofluorescence……11

## List of Symbols/ Nomenclature

1. ADT – androgen deprivation therapy

2. AP – anterior prostate lobe

3. AR – androgen receptor

4. BPH – benign prostatic hypertrophy

5. CARN – castration-resistant Nkx3.1 expressing cell

6. CK4 – cytokeratin 4

7. CK5 – cytokeratin 5

8. CK8 – cytokeratin 8

9. CRPC – castration-resistant prostate cancer

10. IF – immunofluorescence

11. Ki-67 – antigen identified by monoclonal antibody Ki 67

12. $LSC^{med}$ – $Lin^{-}/Sca\text{-}1^{+}/CD49f^{med}$ cells, luminal progenitor profile

13. Nkx3.1 – NK3 homeobox 1

14. Pax2 – paired box 2

15. PSA – prostate-specific antigen

16. Pcsa – prostate stem cell antigen

17. scRNA-seq – single-cell ribonucleic acid sequencing

18. Trop2 – tumor-associated calcium signal transducer 2

19. t-SNE – t-Distributed Stochastic Neighbor Embedding

20. VP – ventral prostate lobe

# Chapter 1: Introduction

Prostate cancer is one of the most common cancers among men worldwide. In 2020 it is projected that prostate, lung, and colorectal cancers will account for 43% of all cancer cases in men in the United States with prostate cancer representing more than 1 in 5 new diagnoses (Siegal et, al., 2020). The symptoms of prostate cancer are very similar to those of benign prostatic hypertrophy (BPH) and include frequent nighttime urination, poor urinary stream, erectile dysfunction, and visible haematuria (Merriel et, al., 2018) so diagnosis based on symptoms alone was difficult and diagnosis of asymptomatic individuals was rare until the widespread use of prostate-specific antigen (PSA) testing beginning in the late 1980s (Welch & Albertson, 2009). Diagnosis is largely reliant on tissue biopsy following the onset of symptoms or high levels of PSA in screening tests. Standard first-line treatments for prostate cancer include surgical intervention by prostatectomy (Kim & Bullock, 2018) or androgen deprivation therapy (ADT) coupled with chemotherapy drugs, and sometimes also coupled with radiotherapy (Litwin & Tan, 2017; Weiner et, al., 2019).

## Prostate Cancer Treatment

ADT is an effective treatment for prostate cancers, as the prostate is highly dependent on androgens. There are various methods of ADT, but the most common are medical castration using gonadotropin-releasing hormone agonists to desensitize receptors that signal the production of testosterone, gonoadotropin-releasing hormone antagonists to decrease the androgen production signals, or inhibitors of steroid synthesis such as inhibitors of 5α-reductase (Sharifi et. al., 2005). Castration by surgical removal of

the testis (orchiectomy) is less common and the reported outcomes state that the 3-year-overall survival rate was only slightly better in patients treated with surgical castration (Sun et. al. 2016). As effective as ADT can be initially reducing the size of the prostate and arresting tumor growth, most patients treated with ADT will eventually develop resistance to the treatment and develop what is called castration-resistant prostate cancer (CRPC or mCRPC if metastatic) even with the continuation of hormone suppression.

Androgen function is mediated by the androgen receptor (AR), which is a member of the nuclear receptor superfamily and a key transcriptional regulator of the prostate (Feng & He, 2019). Castration resistance therefore is dependent on circumventing the requirement of androgen for AR signalling. Limited understanding of prostate cancer's transition from early androgen independence to CRPC indicates changes in the AR signaling pathway in the majority of patients with CRPC. Mechanisms including AR overexpression with or without amplification, AR mutations, AR splice variants, and intratumoral synthesis of androgens have all been observed in CRPC (Huang et, al., 2018). While other pathways such as PI3K-Akt-mTOR have been implicated in CRPC (Statz et, al., 2017), sustained AR signaling is still regarded as the main cause of CRPC and is therefore a subject of many projects looking for ways to target additional pathways in combination with traditional ADT.

**Prostate Anatomy and Histology**

The human prostate is a walnut-sized gland that secretes components of the seminal fluid, and surrounds the urethra at the base of the bladder (Figure 1A). In mice, the prostate has a lobular structure, with 4 pairs of lobes, the anterior, dorsal, lateral, and ventral lobes that branch off of the urethra at the base off the bladder (Figure 1B)

(Toivanen & Shen, 2017). Each of these lobes has characteristic ductal branching patterns.

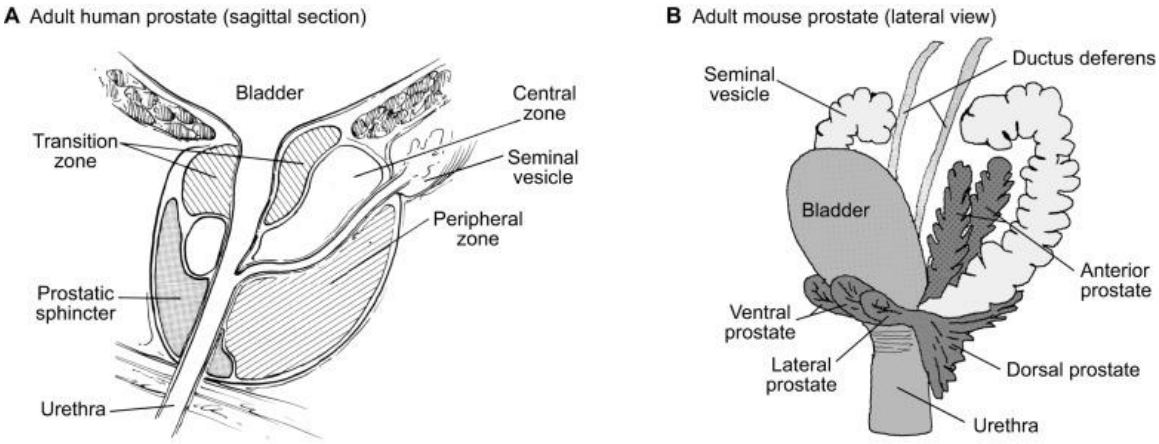


**Figure 1. Anatomy of Human and Mouse Prostate. (**A) Adult human prostate and (B) adult mouse prostate diagrams. Figure adapted from Toivanen & Shen, 2017, McNeal 1969 and Cunha et, al., 1987.

Both the mouse and human prostate epithelium are composed of three differentiated epithelial cell types: luminal, basal, and neuroendocrine (Abate-Shen & Shen, 2000). The luminal epithelial cells are columnar cells lining the lumens in a continuous layer. Luminal cells express high levels of cytokeratin 8 (CK8) and high levels of AR. Basal cells form a layer beneath luminal cells and above the basement membrane. Basal cells express cytokeratin 5 (CK5), but express AR at low or undetectable levels (Toivanen & Shen 2017). Neuroendocrine cells are rare and have undefined function, but express endocrine markers such as synaptophysin (Shen & Abate-Shen, 2010). During puberty, the presence of androgens drives the differentiation of these cell types and expands the luminal cell population. ADT leads to apoptosis of approximately 90% of luminal cells. However, two weeks after re-administration of androgens the prostate will fully regenerate, which indicates that there is a population of stem cells that are castration resistant (Wang et, al., 2009). Earlier work showed that basal cells are largely unaffected

by castration (Tsujimura et, al., 2002), but upon re-administration of androgens following castration an increase in proliferation of $AR^-$ basal cells was detected approximately 48 hours after $AR^+$ luminal cells to experience a small increase in proliferation indicating that androgens have an indirect effect on basal cells despite lack of AR (Mirosevich et, al., 1999). Both luminal and basal prostate progenitors have been identified, and many researchers are seeking to identify and characterize these progenitor cell populations because they can be targets for oncogenic changes that result in tumors that grow even when levels of androgen are low.

**Prostate Luminal Progenitor Populations**

Since prostate cancers display luminal properties, it is possible that stem/progenitor-like cells in prostate cancers may resemble luminal progenitor cells. $Lin^-/Sca\text{-}1^+/CD49f^{med}$ cells ($LSC^{med}$) identified by fluorescence activated cell sorting (FACS) have been shown to have castration-resistant tumor-initiating properties in mouse models prostate cancer (Sala et, al., 2017). Transcriptomic analysis of these cells shows that their gene expression profile shares markers of both basal and luminal cells, which may have prevented previous detection of this population. Sala et, al. identified and validated cytokeratin 4 (CK4) as a specific marker for the $LSC^{med}$ population in both sorted cells and within prostate tissues. This probable source of prostate cancer relapse following castration is certainly a therapeutic target for the prevention of CRPC (Sala et. al. 2017).

Crowell et. al. identified a different population of luminal progenitors by Trop2 expression, while investigating what drives prostate gland expansion and BPH that occurs with age. They reported that luminal prostate cells in old mice express elevated transcript levels of stem and progenitor markers such as *Cd44, Itga2,* and *Tacstd2 (Trop2)* and that

luminal cells from older mice express significantly higher levels of Trop2 than luminal cells from younger adult mice. The $Trop2^{+}$ luminal population included a larger proportion of proliferating cells and were capable of forming larger organoids at a higher rate than the $Trop2^{-}$ population (Crowell et. al. 2019). This pool of progenitor cells is a potential target for oncogenic transformation, though it has not been determined if aged prostate epithelial cells are more susceptible to such transformation.

The $CK4^{+}$ luminal cells described by Sala et, al. are restricted to the proximal region of prostatic lobes in wild-type animals (Sala et. al., 2017) while the $Trop2^{+}$ luminal population described by Crowell et, al. is concentrated in the proximal region, but $Trop2^{+}$ luminal cells are also observed distally in ridges protruding into the luminal duct (Crowell et. al., 2019). The distal prostate also contains Castration-resistant Nkx3.1-expressing cells (CARNS), a population of rare luminal stem cells that express Nkx3-1 in the absence of testicular androgens and function in prostate regeneration (Wang et, al., 2009). Identifying additional markers of progenitor populations in either the distal or proximal prostate is an active area of research.

**Clusterin as Potential Therapeutic Target for Prostate Cancer**

The focus of my thesis is on Clusterin (Clu), which is a highly conserved chaperone protein first discovered in ram rete testis fluid, but is present in many tissues and cancers and is strongly implicated in CRPC (Cochrane et, al.,2007; Wilson & Zoubeidi, 2016). At least two isoforms of Clu are present in mice, caused by transcriptional regulation by AR. Isoforms of Clu are either secretory or nuclear and function as pro-survival or pro-apoptotic, respectively (Cochrane et, al., 2017). In human prostate cancer, secreted Clu levels are correlated with tumor grade (Steinberg et, al.,

1997); overexpression of Clu is associated with high-grade tumors and castration-resistance while the role of nuclear Clu is not as well characterized and expression is associated with cytotoxic events such ionizing radiation (Shannan et, al., 2006). Secretory Clu in mice has also been identified as a marker for loss-of-Nkx3.1 expression by Song et. al, who directly correlated Clu overexpression with Nkx3.1 loss at the cellular level during the initial stages of prostate tumorigenesis, further identifying Clu as a possible key player in cancer development (Song et, al., 2009). Clu has been shown to interact with growth factor receptor signaling pathways involved in oncogenesis/cancer progression such as IGF-1, TGFβ, VEGF, PI3K/AKT, and MAPK (Wilson & Zoubeidi, 2016). This makes secretory Clu a very attractive drug target for prostate cancer treatment. Further mentions of Clu in this thesis refer to secretory Clu unless otherwise specified.

An anti-sense oligonucleotide drug against Clu called OGX-011 or Custirsen, specifically targets the translation initiation site of secreted clusterin (Zoubeidi et, al., 2010) has shown promise in clinical trials. Combining second-generation anti-androgen treatment (enzalutamide treatment) with Clu knockdown by either siRNA or OGX-011 has been found to accelerate AR protein degradation and repress AR transcriptional activity, leading to cell cycle arrest and apoptosis rates higher than either therapy alone (Matsumoto et, al., 2013). A randomized phase II clinical trial studied OGX-011 in combination with docetaxel to treat chemotherapy-naïve mCRPC and concluded that median overall survival using the combination therapy was 7 months longer than using docetaxel alone (Chi et. al. 2010). Due to the success of phase II trials, several phase III studies of OGX-011-chemotherapy combination treatments were conducted. However,

though the results were negative and no survival benefit was recorded for CRPC patients, it was noted that homozygous loss of Clu occurred in 20% of CRPC patients and that this loss of Clu may have contributed to the failure of the phase III trials (Wilson & Zoubeidi, 2017)

It is not known whether Clu marks a progenitor population in the prostate. However, Clu has been shown to mark a population of revival stem cells (revSCs) in the intestinal epithelium that repopulates intestinal crypt bases following injury (Ayyaz et.al., 2019). These unique stem cells are marked by high Clu expression and are very rare during homeostatic conditions but following injury by irradiation or chemical ablation, $Clu^+$ cells undergo a transient expansion to regenerate a functional intestine. RevSCs are also slow-cycling and only undergo expansion as a response to damage before returning to homeostatic numbers (Ayyaz et.al., 2019).

In this study, we investigated the properties of $Clu^+$ cells within the normal mouse prostate during prostate development and following castration and during androgen-mediated regeneration. Using single-cell RNA sequencing (scRNA-seq) data, we assessed prostate tissue cellular heterogeneity and identified *Clu* positive populations throughout prostate development and in the adult prostate. We characterized these *Clu* expressing populations, and conducted immunofluorescence staining to confirm findings from sc-RNA seq and to investigate the localization of cells expressing Clu. We found that Clu is strongly expressed in the proximal region of the prostate as well as in tight clusters in the distal prostate. While $Clu^+$ foci in the distal prostate were less proliferative, they appeared to be dependent on androgens as these foci were not detected at early developmental timepoints or in the fully regressed prostate.

# Chapter 2: Methods

## Mouse strains

Swiss Webster wildtype mice were obtained from Taconic. C57BL6 mice were obtained from the Jackson Laboratory.

## Mouse procedures and surgery

Adult male mice aged 7-8 weeks were castrated using standard techniques. For prostate regeneration testosterone propionate (Sigma T-1875) was dissolved at 25 mg/mL in 100% ethanol and diluted with PEG-400 to final concentration of 7.5 mg/mL. Mini osmotic pumps (Alzet 1002) implanted subcutaneously were used to administer testosterone for up to 2 weeks at a rate of 1.875 µg/h to achieve physiological levels of serum testosterone. All animal experiments received approval from the Institutional Animal Care and Use Committee at the George Washington University. Mouse experiments were not randomized.

## Tissue collection and prostate dissociation

For IF analyses, both individual prostate lobes and whole prostates were dissected and fixed in 4% paraformaldehyde followed by cryo-embedding in OCT compound (Sakura). Tissue samples obtained from 1W, 3W, and 4W mice were dissected and fixed as whole prostates. Other 4W samples and samples from castrated fully regressed mice and 3-day, 7-day, or 2-week regenerating mice were dissected into anterior, ventral, and dorsal-lateral lobes.

Prostate tissues from C57BL6 mice were dissected and minced into small clumps and then enzymatically dissociated with 300 U/mL collagenase, 100 U/mL hyaluronidase

(StemCell Technologies 07912) diluted in hepatocyte culture media (Corning 355056) with 5% FBS (Invitrogen) for 1 h at 37ºC before being washed with Hanks' Balanced Salt Solution(HBSS)/10 mM HEPES/2% FBS and resuspended in TrypLE Express Enzyme (Gibco 12605010) and incubated for 10 min at 37ºC. Samples were washed with HBSS/HEPES/FBS and then resuspended in prewarmed 5mg/mL Dispase/ 1 mg/mL DNaseI solution for 1 min. Samples were washed and resuspended with HBSS/HEPES/FBS and filtered through a 40 μm cell strainer (StemCell Technologies 27305) before a small amount of cells were stained with Trypan Blue and counted using a Countess II FL Cell Counter. Single cell suspension was then used for organoid culture.

**Prostate organoid culture**

Prostate organoids were generated using frozen organoids from EpCAM-sorted cells from C57BL/6 mice. These cells were thawed and plated in floating culture medium, as described by Chua et. al. 2014. Medium was prepared by adding the following components to hepatocyte medium, EGF (10 ng/mL), heat inactivated charcoal-stripped FBS (to 5% final concentration), GlutaMAX (100 × diluted), Matrigel (to 5% final concentration), ROCK inhibitor Y-27632(10μM) (StemCell Technologies), DHT ($10^{-7}$M). Organoid culture medium was warmed before being added to the 96-well low attachment plates (Corning 07200603). Medium was added every 4-5 days. After 3 weeks of growth, organoids were passaged by treatment with TripLE for 5 minutes followed by resuspension and plating with organoid culture medium. Organoids used for immunofluorescence staining were collected at day 21 of passage 1. Organoids were treated with 5 mg/mL dispase in hepatocyte medium for 30 min at 37ºC to remove Matrigel before being spun down, washed with PBS, and resuspended with 4% PFA for

30 minutes for fixation. After fixation, organoids were placed in 30% sucrose and embedded in OCT.

**Immunofluorescence staining**

For OCT-embedded tissues and organoids, 8 µm sections were heated in citric acid based Antigen Unmasking Solution (Vector Labs) until boiling before they were blocked with 10% normal donkey serum (NDS) for 1 h and incubated with primary antibodies diluted in 5% NDS overnight at 4ºC. Samples were incubated with secondary antibodies (diluted 500-fold in 5% NDS) labeled with Alexa Fluor 488, 555, or Dylight 550 (Invitrogen) at room temperature for 1 h. DAPI stain was applied to sections for 5 min. Slides were mounted with Vectashield mounting media (Vector Labs) or equivalent. Imaging was conducted on a Leica DMi8 A microscope. All primary antibodies and dilutions used are listed in Table 1.

**Single-cell RNA sequencing data analysis**

Previously obtained single-cell RNA sequencing data generated using the 10X Genomics platform (M Shibata and M Shen, unpublished) was analyzed using the Loupe Cell Browser. Single-cell RNA-seq data from postnatal day (p) 0, 1-, 4-, and 10-week (W) data was displayed in t-SNE plots. The Gene/Feature Expression menu was used to display expression of individual genes in the t-SNE chart, color coded light orange for lowest Log2 expression value to dark red for highest Log2 expression value.

**Cell counting**

Cell numbers were manually counted using 20x images of tissue sections. $Clu^{+}$ cells were analyzed by counting the Ki-$67^{+}$and Ki-$67^{-}$ cells within 2 large proximal areas and 4 small distal areas from one 4-week-old animal. Values were expressed as the

percentage of $Clu^+$ cells counted in either the proximal or distal regions. Data was plotted using GraphPad Prism 8 and statistical analysis was run using Statistics Calculator from StatPac. One sample t-test between percents was performed for the proximal data.

Table 1. Information of antibodies used for immunofluorescence

| **Primary Antibodies** | | | |
|---|---|---|---|
| **Antibody** | **Supplier** | **Product Number** | **Dilution** |
| AR | Abcam, Cambridge, UK | ab133273 | 1:100 |
| CK5 | Biolegend, San Diego, CA | 905501 | 1:500 |
| Clusterin | R&D systems, Minneapolis, MN | AF2747 | 1:200 |
| Ki-67 | eBioscience, Inc., San Diego, CA | 14-5698-80 | 1:1000 |
| Nkx3.1 | AthenaES, Baltimore, MD | 315 | 1:500 |
| **Secondary Antibodies** | | | |
| **Antibody** | **Supplier** | **Product Number** | **Dilution** |
| Donkey Anti-Goat Alexa Fluor 488 | Thermo Fisher Invitrogen, Waltham, MA | A-11055 | 1:500 |
| Donkey Anti-Rabbit Alexa Fluor 555 | Thermo Fisher Invitrogen, Waltham, MA | A31572 | 1:500 |
| Donkey Anti-Rat Dylight 550 | Thermo Fisher Invitrogen, Waltham, MA | SA5-10027 | 1:500 |

# Chapter 4: Results

## *Clu* Expression in Cells in the Developing and Adult Prostate

To investigate the expression of *Clusterin (Clu)* in the developing prostate, we analyzed scRNA-seq data from postnatal day (p) 0, 1-, 4-, and 10-week (W) prostates. Data from each time point was visualized on a t-SNE plot which clusters cells according to similarities in their gene expression. *Clu* expression was observed in all developmental timepoints and in the adult prostate, with some populations of cells expressing higher levels. At p0 and 1W, *Clu* expression was either not detected or low in most cells (Figure 2A, B respectively). Populations with higher *Clu* expression were observed in the developing prostate at 4W (Figure 2C) and in the adult prostate at 10W (Figure 2D).

Given that *Clu* is known to be expressed in seminal vesicles (Grima et. al.,1990), we examined the expression of *Pax2*, a marker for seminal vesicle cells (Kuschert et, al., 2001). A clearly defined population of $Pax2^{+}$ cells was observed across developmental timepoints and in the adult prostate (Figure 2A-D). Each $Pax2^{+}$ population expressed high levels of *Clu*. However, the $Clu^{+}$ cells that did not express *Pax2* at p0 and 1W were not tightly clustered though clearly defined $Clu^{+}/Pax2^{-}$ were detected at 4W and 10W with stronger Clu expression.

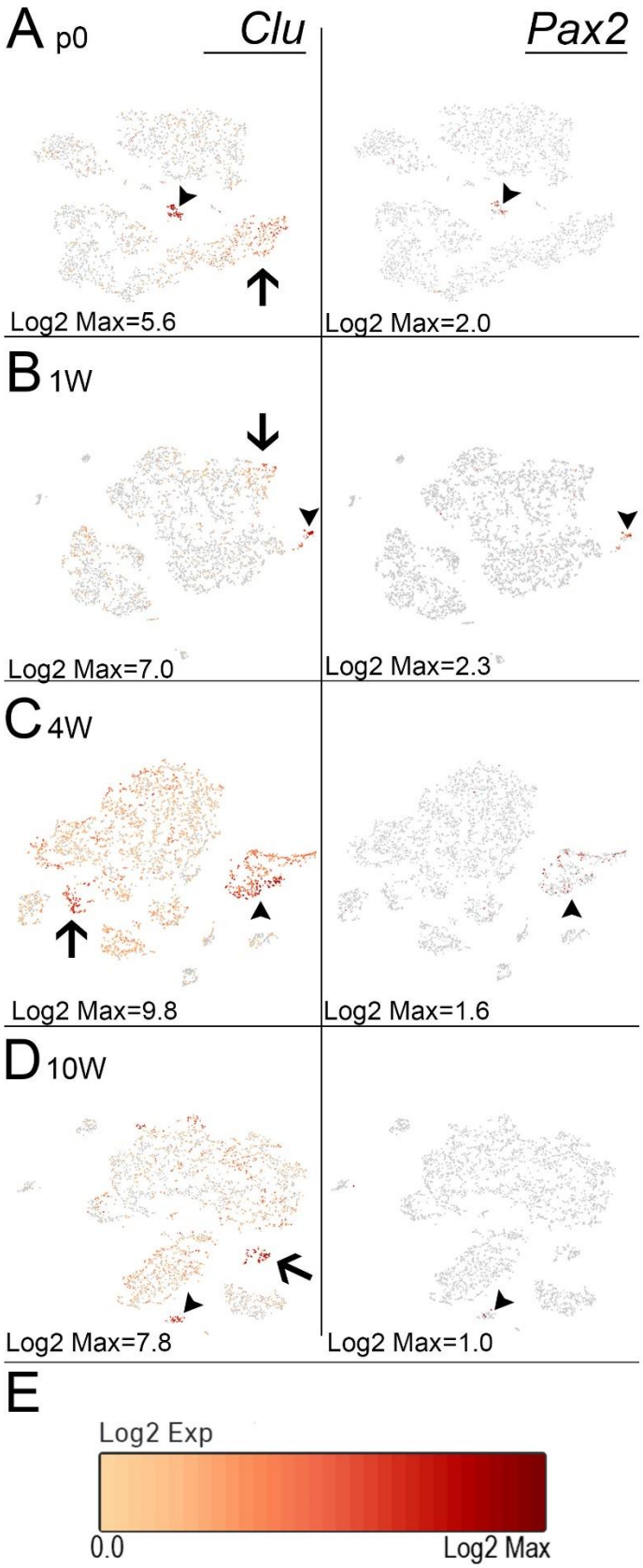


**Figure 2. scRNA-seq data highlighting *Clu* expression.** (A-D) t-SNE plots generated from scRNA-seq data showing expression of *Clu* and seminal vesicle marker *paired box 2 (Pax2)*. Postnatal day (p) 0, 1-, 4-, and 10 week (W) prostate data are shown. Each dot represents a single cell. (I)Log2 expression is represented by color gradient; light orange representing lowest expression and dark red representing highest expression. Arrows point to regions of $Clu^{+}$ luminal epithelial cells. Arrowheads point to regions of $Pax2^{+}$ seminal vesicle cells, which are known to express high levels of Clu. $Pax2^{+}$regions are not investigated in this study.

### *Clu*$^+$ Cluster at 4W is Likely Luminal and Proximal

To further characterize the *Clu*$^+$ population identified at 4W (Figure 2C) we analyzed the expression of luminal and basal markers in this population. *Clu*$^+$ prostate cells from 4W prostates (Figure 2C) expressed high levels of *Tacstd2* (Figure 3B) and *Psca* (Figure 3C) which are highly enriched in the proximal prostate (Crowell et, al., 2019) and *CK4* (*Krt4)* (Figure 3D), which in wild-type animals is restricted to the proximal region of prostatic lobes (Sala et. al., 2017). The proximal region of the mouse prostate is directly adjacent to the urethra and is known to contain many stem-like cells that are quiescent, have high proliferative potential, and are pluripotent (Goto et. al., 2009).

*Clu*$^+$ prostate cells did not express *CK5 (Krt5),* a basal cell marker (Figure 3E) but expressed high levels of *CK8 (Krt8),* a luminal cell marker (Figure 3F). Expression of *Nkx3.1* (Figure 3G), which is expressed in luminal cells of the distal prostate (Bahatia-Gaur et. al.,1999), was low in *Clu*$^+$ prostate cells. Expression of Ki-67 (*Mki67),* a proliferation marker (Scholzen and Gerdes, 2000), was also low in *Clu*$^+$ prostate cells (Figure 3H). In summary, these findings suggest an enrichment of *Clu*$^+$ prostate cells with luminal properties in the proximal region of the prostate.

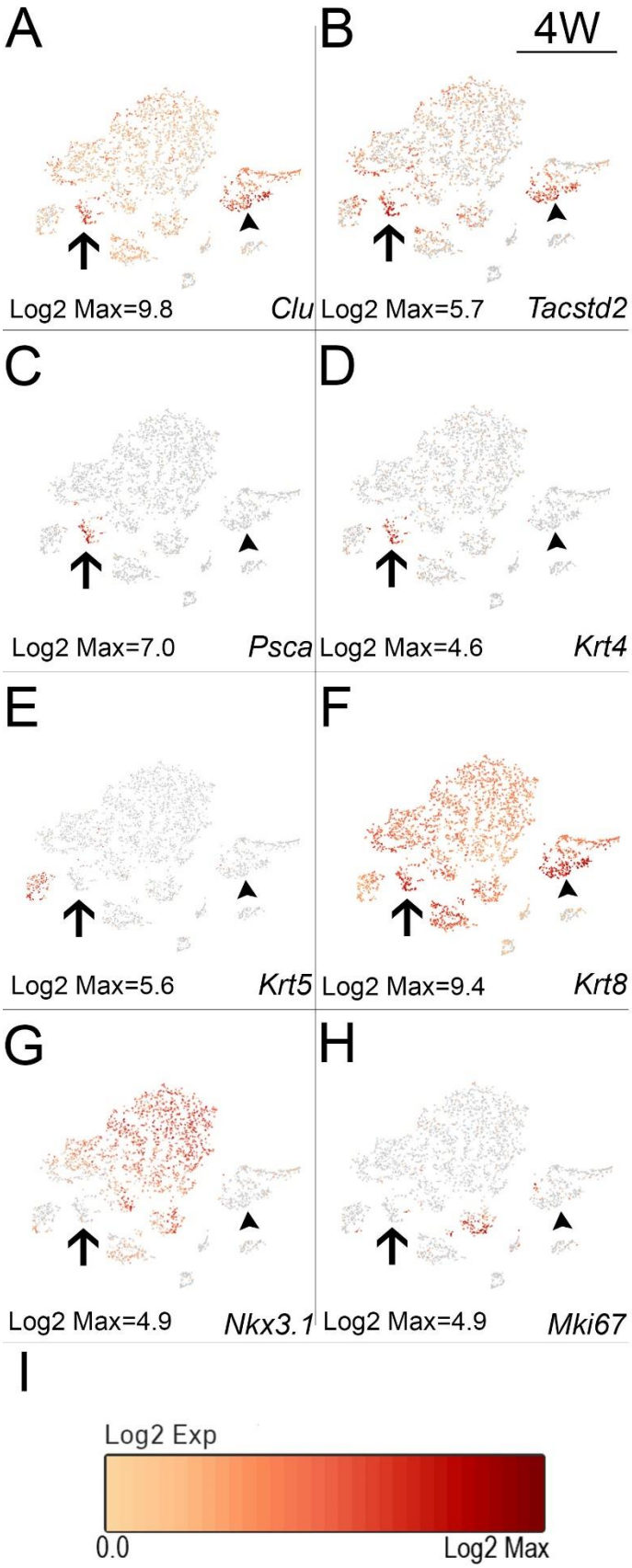


**Figure 3. *Clu* expression at 4W compared to proximal, basal, luminal, and proliferative markers. (**A-H) t-SNE plot generated using scRNA-seq data from prostates at 4W. Each dot represents a single cell. . (I)Log2 expression is represented by color gradient; light orange representing lowest expression and dark red representing highest expression. (A) *Clusterin (Clu),* (B) proximal marker *tumor-associated calcium signal transducer 2 (Tacstd2),* (C) proximal marker *prostate stem cell antigen (Psca),* (D) proximal marker *CK4 (Krt 4),*(E) basal marker *CK5 (Krt5),* (F) luminal marker *CK8 (Krt 8),* (G) distal marker *NK3 homeobox 1 (Nkx3.1),* and (H) proliferation marker *antigen identified by monoclonal antibody Ki 67 (Mki67)* expression is used to characterize $Clu^+$ cells. Arrows point to regions of $Clu^+$ luminal epithelial cells. Arrowheads point to regions of $Pax2^+$ seminal vesicle cells.

## Changes in Clu Expression Across Prostate Development

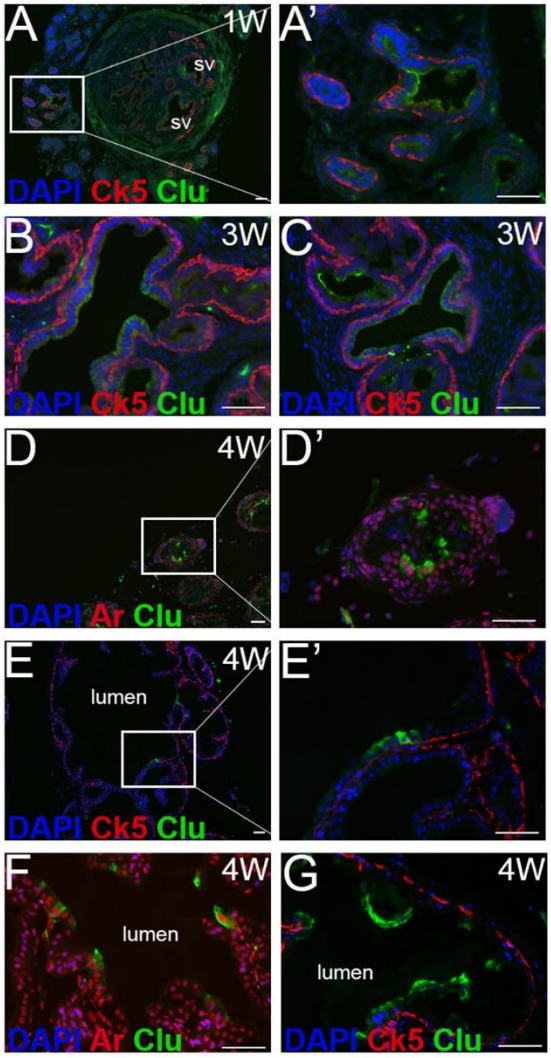


**Figure 4. Immunofluorescent staining for Clu in neonatal, prepubescent, and pubescent mice.** Immunofluorescence images of prostate lumens in (A) 1 W whole prostate, (B)3- and (D-G) 4- W developing AP lobes. (A', D', and E') Higher magnification images of areas highlighted by white boxes. Staining for Clu (green), Ck5 or AR (red), and DAPI (blue) is shown merged in each image. Scale bars, 50 µm. Images of p7 and 3W prostates were obtained from one animal at each timepoint.SV, seminal vesicle

$Clu^+$ luminal cells have been detected in the distal prostate and as a continuous layer in the proximal region in wild type mice of 4-5 weeks of age (Korsten et. al. 2009). Given the changes in *Clu* RNA expression that we observed throughout prostate development, we hypothesized that Clu expression would be low in early development but high in puberty, especially in the proximal region. To determine the localization of $Clu^+$ cells, we conducted immunofluorescence (IF) co-staining for Clu, CK5 and Androgen Receptor (AR), which has been shown to be a transcriptional regulator of Clu (Cochrane et. al. 2007). We detected Clu expression in prostate lobes examined at 1W, 3W and 4W of age (Figure 4). At 1W, Clu expression was cytoplasmic, and was weak but continuous around the entire prostate lumen (Figure 4A, n= 1 animal). The low

Clu expression in a continuous layer of cells was also observed in prostates at 3W (Figure 4B, n=1 animal).

In 4W prostate tissue, we detected two patterns of Clu expression. In one pattern, cells expressing high levels of Clu were observed as tight clusters of approximately 4-6 cells surrounding lumens (Figure 4D), at the tips of tufts (Figure 4F), or along smooth areas of lumen (Figure 4E). In another pattern, Clu was expressed in groups of more than 6 cells, as longer stretches of cells lining the lumen (Figure 4G). At this stage of prostate development, $CK5^+$ basal cells were observed at an approximately 1:1 ratio with luminal cells. $Clu^+$ cells did not express CK5 and were located in the luminal layer of the prostate duct. Co-staining with AR revealed that some $Clu^+$ cells expressed higher levels of AR than surrounding $AR^+$ cells (Figure 4D, 3F). The high level of Clu expression in a small number of cells throughout the prostate at 4W was notably different compared to the low continuous expression around the lumen at 3W.

**Clu Expression in the Regenerating Prostate Resembles that of the Developing Prostate**

Clu is expressed in regenerating stem cells in the intestinal epithelium, which are rare under homeostatic conditions but undergo transient expansion to repopulate the intestinal crypt base following injury (Ayyaz et. al.,2019). To determine if Clu has similar functions during prostate regeneration, we evaluated Clu expression during prostate regeneration by castrating mice and then assessing Clu expression after treating the mice with androgens (Figure 5A). Mature males (7-8 weeks old) were surgically castrated and fully regressed prostates were collected after 4 weeks (n=2 animals). We

conducted IF staining for Clu, AR, and CK5 and found that in regressed prostates, Clu expression was weak, cytoplasmic, and was continuous around the entire lumen (Figure 5 B,C n=1 animal) similar to the staining observed in the 1W normal prostate (Figure 4A). AR expression was cytoplasmic in luminal cells of the fully regressed prostate, as expected (Tan et. al., 2014).

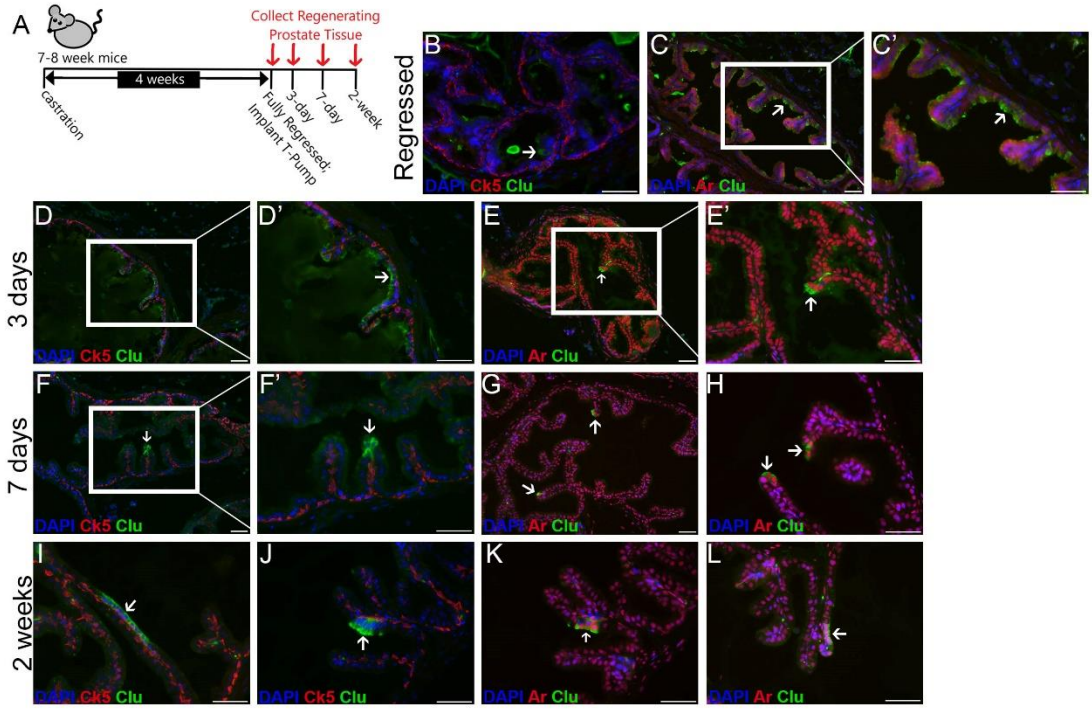


**Figure 5. Clu expression in regressed and regenerated prostates.** (A) Experimental timeline for castration and androgen-mediated regeneration. Immunofluorescence staining images of anterior prostate lobes (B-C) fully regressed, (D-E) regenerated for 3 days , (F-H) regenerated for 7 days, and (I-L) regenerated for 2 weeks. Staining for Clu (green), Ck5 or AR (red), and DAPI (blue) is shown merged in each image. Scale bars, 50 µm. (C', D', E', and F') higher magnification images of areas highlighted by white boxes. Arrows indicate $Clu^+$ cells.

We then implanted Testosterone pumps in the castrated mice to induce prostate regeneration (Figure 5A, n=9 animals). At 3 days of regeneration, we detected two different patterns of Clu expression in the prostate. We observed low levels of Clu expressed in a continuous stretch of cells along the lumen (Figure 5D), similar to what we observed in the regressed prostate (Figure 4C). We also observed tight clusters of

approximately 3-6 $Clu^+$ cells at the tips of tufts (Figure 5E). This focal pattern of expression was also observed in the 4W prostate (Figure 4F). Focal expression of Clu was also detected at day 7 of regeneration (Figure 5F, G, H) and at 2 weeks of regeneration (Figure 5J, K, L). $Clu^+$ cells co-expressed nuclear AR during prostate regeneration (Figure 5E, G, H, K, L). We did not detect obvious differences in the expression pattern of Clu at day 3, day 7 and 2 weeks of regeneration. These findings suggest similarities in the role of Clu during prostate development and regeneration.

**Comparison of Clu Expression in the Proximal and Distal Prostate**

To confirm findings from our analysis of scRNA-seq data which indicated that $Clu^+$ cells express markers for the proximal prostate (Figure 3), we stained 4W prostate tissues for Clu and Nkx3.1, which is not expressed in proximal prostate cells (Bahatia-Gaur et. al.,1999). Near the urogenital sinus (UGS), we observed prostate cells that expressed Clu but not Nkx3.1 (Figure 6A1, A2). We also observed that cells near the proximal prostate that expressed Nkx3.1 did not express not Clu (Figure 6A1, A2). Clu was strongly expressed in the cytoplasm of the proximal luminal cells while Nkx3.1 staining was nuclear. In prostate lobes at 7 days of regeneration, we also identified luminal cells in the proximal prostate that expressed high levels of cytosplasmic $Clu^+$ and luminal cells that expressed nuclear Nkx3.1 but not Clu (Figure 6B, C).

In distal prostate, small clusters of $Clu^+$ cells were observed at the tips of tufts. Intriguingly, cells in some of the distal clusters co-expressed Nkx3.1 and Clu (Figure 6E, n=4 clusters) whereas cells in other $Clu^+$ clusters did not express Nkx3.1 (Figure 6D, n=2 clusters). Cells co-expressing Clu and Nkx3.1 were columnar shaped (Figure 6E, n=4

clusters) while the cells expressing Clu alone were tightly bunched and appeared teardrop shaped (Figure 6D, n=2 clusters). These results indicate that Clu is a marker for proximal cells in the prostate during puberty and in the regenerating prostate. Furthermore, our

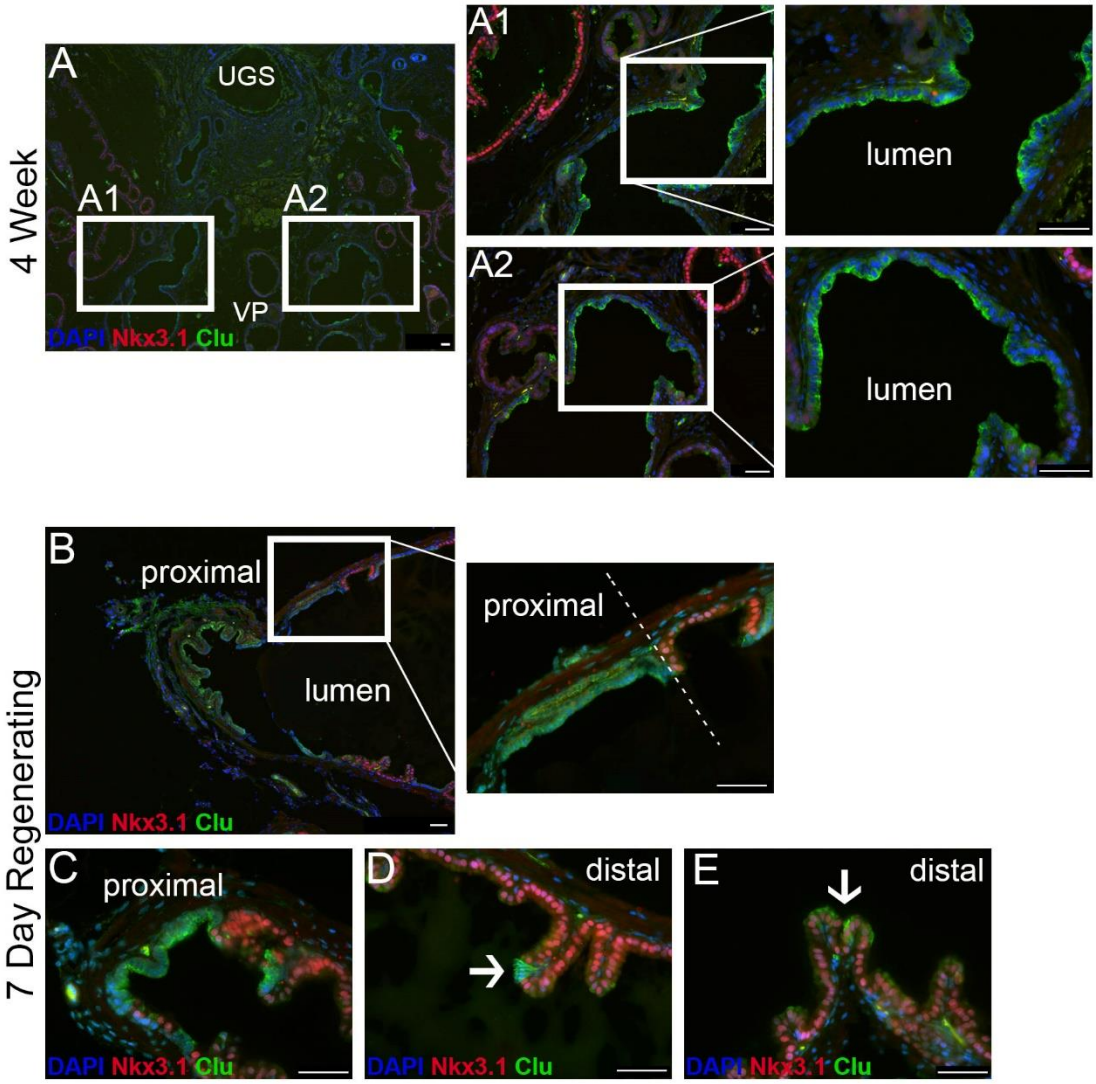


**Figure 6. Clu expression in the proximal and distal prostate.** Immunofluorescence images of (A) 4W ventral prostate (VP), and (B-E) anterior prostate (AP) 7 days after androgen-mediated regeneration. Staining for Clu (green), Nkx3.1 (red), and DAPI (blue) is shown merged in each image. Scale bars, 50 μm. Arrows indicate $Clu^+$ cells in distal lumens. Lower magnification images included to show areas of localization in tissue.

findings suggest the presence of two different $Clu^+$ populations in the regenerating distal prostate: one that does not express Nkx3.1 and resembles the proximal prostate, and one that expresses Nkx3.1.

## Reduced Proliferation in Clu$^+$ Cells in the Distal Prostate

To determine if Clu expression is associated with proliferation, we performed IF staining for Ki-67 with co-staining for Clu. The Ki-67 protein is only expressed in actively dividing cells and is commonly used to measure proliferation (Scholzen and Gerdes 2000). In prostates from 4W animals, many cells expressing Ki-67 (Ki-67$^+$) were

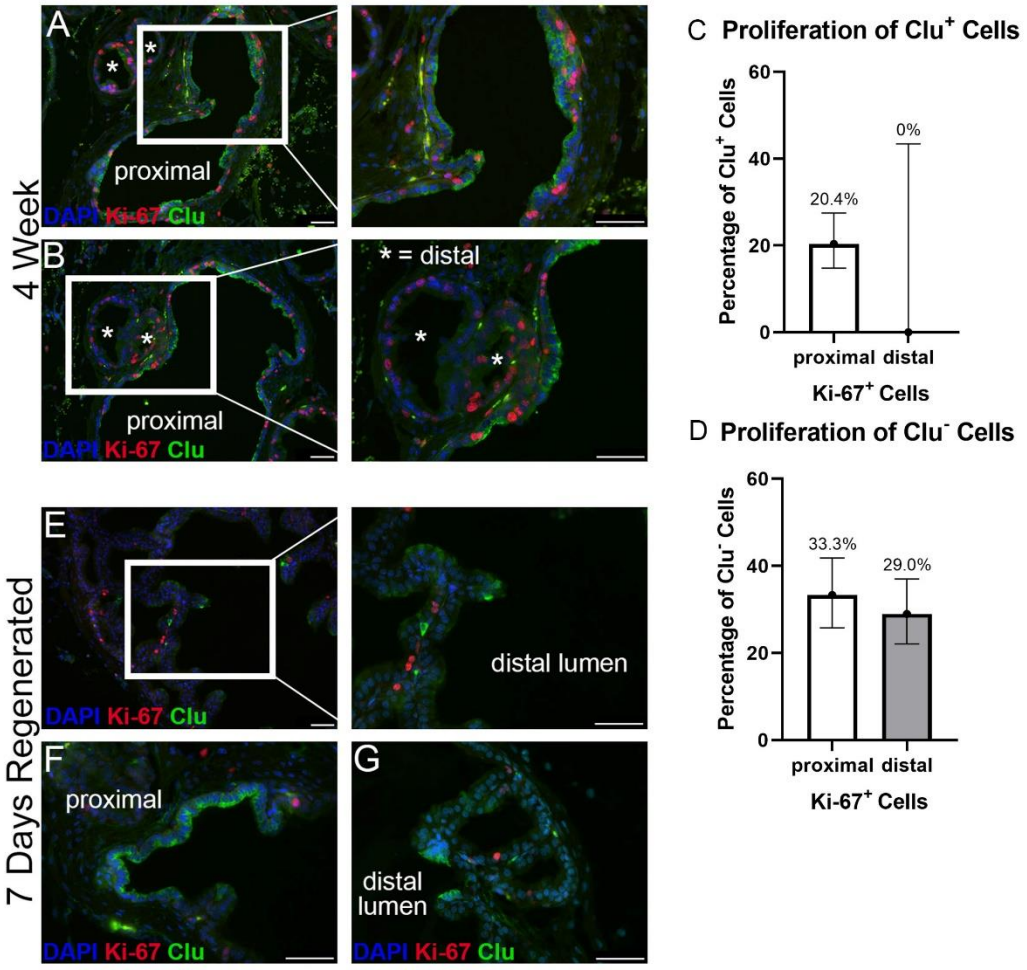


**Figure 7. Immunofluorescence co-staining for Clu and Ki-67 proliferation marker.** (A, B) Immunofluorescence images of proximal and distal regions of ventral prostates (VP) from 4W mice. Staining for Clu (green), Ki-67 (red), and DAPI (blue) is shown merged in each image. (C) Percentage of Clu$^+$ cells that co-express Clu and Ki-67 and those that express Clu alone in proximal and distal lumens of 4W VP. P=0.0000, one sample t-test between percents (D) as in C with Clu$^-$ cells, P=0.9510, not significant (E-G) As in (A) with 7 days regenerated AP. Scale bars, 50 µm.

observed (Figure 7 A, B). We counted the number of Clu$^+$ luminal cells that were Ki-67$^+$ and Ki-67 negative (Ki-67$^-$) in both proximal and distal areas of one 4W prostate. There

were no Ki-67$^+$ cells detected in distal areas, and in the proximal areas, only 20.4% of Clu$^+$ cells expressed Ki-67 (Figure 7C, n=152 Clu$^+$ proximal cells, 5 Clu$^+$ distal cells) indicating that proliferation is not enriched in Clu$^+$ proximal cells. Clu$^-$ cells did not show any differences in proliferation between proximal and distal regions (Figure 7D, n=129 Clu$^-$ proximal cells, 138 Clu$^-$ distal cells). At 7 days of regeneration, there were very few proliferating cells in either the proximal or distal regions. Co-expression of Clu and Ki-67 was not detected in either the distal (Figure 7E, G) or the proximal region (Figure 7F) at 7 days of regeneration.

**Clu Expression in Organoids**

Since organoid culture allows for the growth of prostate luminal cells in 3D culture conditions (de Souza 2017, Chua 2014), we generated prostate organoids to evaluate Clu expression in cultured prostate luminal cells (Figure 8A). We then conducted IF staining for Clu and AR. We detected 2 types of organoids. One type of organoid expressed nuclear AR and did not express Clu (Figure 8B-E, n=4 organoids). The second type of organoid co-expressed AR and Clu (Figure 8F-I, n =1 organoid). Surprisingly, Clu expression was nuclear, in contrast to cytoplasmic expression observed in the prostate *in vivo*. Nuclear Clu is associated with programed cell death (Cochrane et, al., 2007) and may indicate that the Clu$^+$ organoid was dying. Debris in the lumen of both organoid types stained positive for Clu.

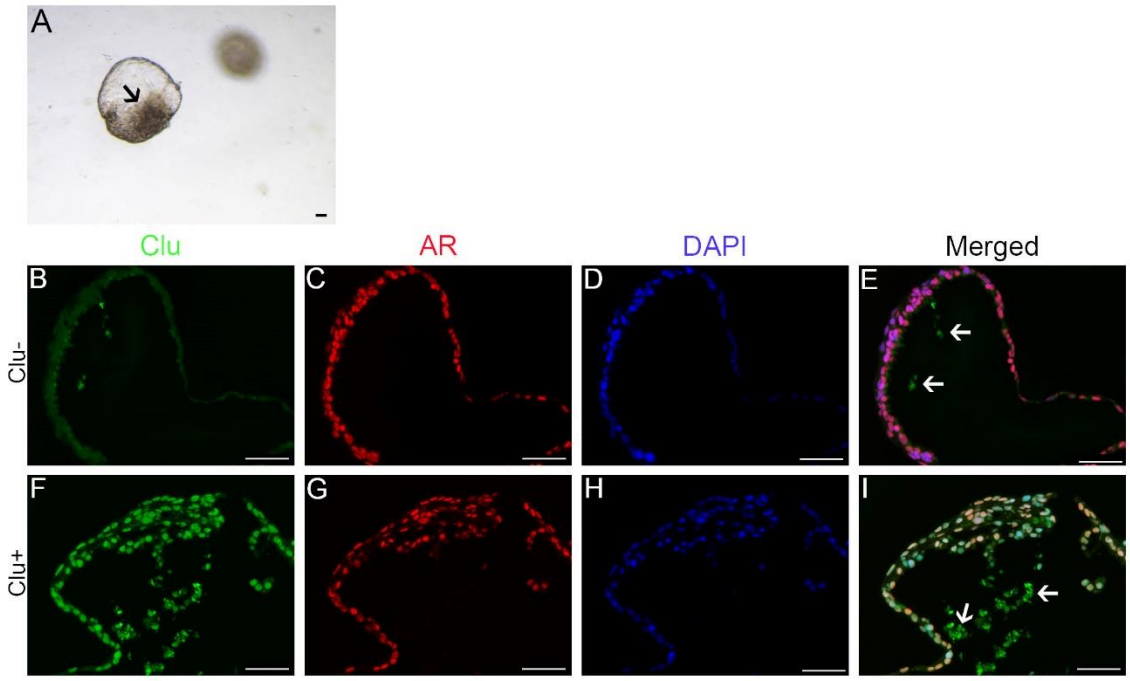


**Figure 8. Immunofluorescence staining of luminal organoids grown in 3D culture conditions.** (A) Brightfield image of C57BL/6 luminal organoid growing at passage 1 for 21 days. (B-E) Representative immunofluorescence images of C57BL/6 organoids growing at passage 1 for 21 days. Staining for Clu (green), AR (red), and DAPI (blue) is shown individually and merged. Scale bars, 50 µm. (F-I) Image of a rare $Clu^{+}$ organoid, stained as described for (B-E). Arrows identify cell debris. Scale bars, 50 µm.

# Chapter 5: Discussion

The function of Clusterin (Clu) in the prostate is not well understood, though Clu has been implicated in cancer progression and in castration resistance (Wilson & Zoubeidi, 2017). In this study, we characterized Clu expression in the normal prostate and found that Clu is highly expressed in subsets of cells in the presence of androgens during puberty and during regeneration. Our findings indicate that Clu expression is affected by levels of androgen. We propose that Clu-expressing cells in the proximal and distal prostate represent separate sub-populations of cells, as they differ in expression of Nkx3.1 and a proliferative marker, Ki-67.

## Characterization of the *Clu*$^+$ Population of Prostate Cells with scRNA-seq

Our analysis of single-cell RNA sequencing (scRNA-seq) data indicates that *Clu* expression is low when levels of circulating androgens are low prior to puberty (Abate-Shen & Shen, 2000). Although we did not detect distinct populations of *Clu*$^+$ cells at p0 and 1W, we observed populations of cells with high *Clu* expression as levels of androgen increased.

*Trop2* (*Tacstd2)*, *Psca,* and *CK4(Krt4)* are expressed in the proximal prostate and are also considered markers of luminal progenitor cells in the prostate (Crowell et, al., 2019; Sala et, al., 2017). The co-expression of *Clu, Trop2, CK4,* and *Psca* in distinct clusters of cells suggests that this population represents cells with stem cell-like properties in the proximal prostate. This was supported by the finding that *Clu*$^+$ cells in the proximal prostate also expressed low levels of *Nkx3.1*, which we confirmed by immunofluorescence (IF) staining for Clu and Nkx3.1.

**Clu Expression in the Distal Prostate is Mediated by Androgens**

Though our scRNA-seq screening suggested that *Clu*$^+$ cells are enriched in the proximal prostate, we also detected Clu expression in the distal prostate. At 4W, these Clu-expressing cells were in tight clusters of approximately 4-6 cells surrounding lumens, at the tips of tufts, or in many cells along the lumen (Figure 3). Clu expression at the tips of tufts and in many cells along the lumen was also detected in the regenerating prostate (Figure 4). Although a similar expression pattern for Clu at the tips of tufts has previously been reported (Korsten et, al., 2009), our findings indicate that Clu is also expressed in larger clusters of cells in the distal prostate. This difference may be attributable to the increased sensitivity of our IF method compared to immunohistochemical staining.

At 3W, prior to puberty, we observed low levels of Clu expression in most prostate luminal cells (Figure 3B), similar to what was detected in the regressed prostate (Figure 4C). The differences in Clu expression between regressed, 3W, and 4W timepoints may be due to differences in levels of androgen, which are low in regressed prostates and at 3W, whereas by 4W of age, androgen levels have increased in the mouse.

During all timepoints examined, we detected cytoplasmic Clu expression, suggesting that the pro-survival secretory isoform of Clu is expressed in the prostate (Cochrane et, al., 2007; Moretti et, al., 2007). The polyclonal anti-Clu primary antibody used in IF stainings was produced using a nearly full-length portion of the Clu protein as immunogen (Table 1), so the cellular localization was integral in determining the isoform of Clu we observed because the antibody detects all Clu isoforms. Our finding that Clu$^+$ cells expressed higher levels of AR than surrounding AR$^+$ cells (Figure 3D, 3F) further

supports that high expression of Clu in the distal prostate occurs in response to androgens.

**Comparison of Clu Expression in the Proximal and Distal Prostate**

Whereas Clu-expressing cells in the proximal prostate did not express Nkx3.1, we observed $Clu^+$ foci in the distal prostate at 7 days of regeneration that co-expressed Nkx3.1 and Clu (Figure 5E), and foci that did not express Nkx3.1 (Figure 5D) similar to proximal cells. Expression of proximal markers such as Trop2 and Psca have been reported in the distal prostate in wild-type animals (Crowell et, al., 2019), though further studies are needed to determine the molecular differences in cells expressing Clu in the proximal and distal prostates. The differences in morphology and Ki-67-expression of $Clu^+$ distal cell populations suggest that Clu-expressing cells in the distal regenerating prostate may have distinct properties.

**Proliferation was Reduced in Clu Expressing Cells in the Distal Prostate.**

During intestinal regeneration, Clu is expressed in stem cells in the intestinal epithelium (Ayyaz et. al., 2019). $Clu^+$ intestinal stem cells are rare under homeostatic conditions but undergo transient expansion to regenerate the intestinal crypt base following injury (Ayyaz et. al., 2019). Similarly, we found that Clu expression increased during prostate development as well as during prostate regeneration. Despite the increase in Clu expression, we did not observe a higher percentage of proliferation in $Clu^+$ cells. However, there were limitations due to the sample size of our studies. It is possible that $Clu^+$ cells are quiescent reserve stem cells that give rise to rapidly diving transit-amplifying cells, though this remains to be investigated. Such slow-cycling transit-

amplifying cells have previously been identified by BrdU-labelling in clusters at the tips of tufts (Tsujimura et, al., 2002) similar to the $Clu^+$ cells we detected in the distal prostate. It is also possible that there are differences in the response of Clu-expressing cells to androgens during androgen-mediated regeneration compared to an injury-mediated model of regeneration. A previous study has concluded that Clu is not critical for prostate regeneration (Fink et. al. 2006), and thus further studies are needed to determine the functional significance of Clu in prostate distal cells.

**Expression of Clu in Organoids Could Not be Determined.**

Organoid culture can be used to evaluate progenitor properties of cells (Crowell et. al., 2019; Chua et, al., 2014) However, we were unable to detect Clu expression in prostate organoids. It is possible that the treatment of organoids with dispase to remove residual Matrigel from the culture media may have affected Clu expression or stressed the organoids and induced apoptosis in cells. Dissociation of prostates from developmental timepoints or from proximal organoids may yield organoids with higher numbers of $Clu^+$ cells. The evaluation of Clu expression in organoids will require further optimization of culture and staining conditions.

In summary, we have confirmed that Clu is expressed in an androgen-dependent manner in both the proximal and distal region of the prostate. We identified distal $Clu^+$ cells that co-expressed Nkx3.1 and distal $Clu^+$ cells that lacked Nkx3.1 which were more similar to proximal cells, suggesting that there are at least two subtypes of $Clu^+$ cells in the distal prostate. Furthermore, our preliminary analysis suggested that $Clu^+$ cells in the distal prostate were associated with reduced proliferation. We hypothesize that these cells

could be quiescent stem cells, though a larger sample size is needed to confirm the reduced proliferation.

Clu inhibition by a small molecule, OGX-011, or by using siRNA in combination with chemotherapy has been shown to be effective for treatment for prostate cancer (Wilson 2016). Other groups have proposed expression profiles for progenitor cell populations that include Clu (Korsten et, al., 2009; Ayyaz et, al., 2019) though our findings indicate that Clu could be expressed in distinct populations of cells or in cells of different states. Future studies focused on co-staining of Clu with other markers including Trop2, Psca, CK4, and Sca-1 (Crowell et, al., 2019; Sala et, al., 2017; Korsten et, al., 2009) would be informative for further investigating the $Clu^+$ populations we have identified in this study. Lineage tracing of $Clu^+$ cells in the distal prostate using BrdU labeling to conduct a pulse-chase analysis (Tsujimura et, al., 2002) would also provide information on the cell fate of $Clu^+$ cells. Clu continues to be an attractive drug target to combat castration-resistant prostate cancer and it is our hope that our findings will provide further insight into the role of Clu in prostate cancer.

References

Abate-Shen, C., & Shen, M. M. (2000). Molecular genetics of prostate cancer. In *Genes and Development* (Vol. 14, Issue 19, pp. 2410–2434). Cold Spring Harbor Laboratory Press. https://doi.org/10.1101/gad.819500

Ayyaz, A., Kumar, S., Sangiorgi, B., Ghoshal, B., Gosio, J., Ouladan, S., Fink, M., Barutcu, S., Trcka, D., Shen, J., Chan, K., Wrana, J. L., & Gregorieff, A. (2019). Single-cell transcriptomes of the regenerating intestine reveal a revival stem cell. *Nature*. https://doi.org/10.1038/s41586-019-1154-y

Bhatia-Gaur, R., Donjacour, A. A., Sciavolino, P. J., Kim, M., Desai, N., Young, P., Norton, C. R., Gridley, T., Cardiff, R. D., Cunha, G. R., Abate-Shen, C., & Shen, M. M. (1999). Roles for Nkx3.1 in prostate development and cancer. *Genes & Development*, *13*(8), 966–977. https://doi.org/10.1101/gad.13.8.966

Chua, C. W., Shibata, M., Lei, M., Toivanen, R., Barlow, L. J., Bergren, S. K., Badani, K. K., McKiernan, J. M., Benson, M. C., Hibshoosh, H., & Shen, M. M. (2014). Single luminal epithelial progenitors can generate prostate organoids in culture. *Nature Cell Biology*, *16*(10), 951–961. https://doi.org/10.1038/ncb3047

Cochrane, D. R., Wang, Z., Muramaki, M., Gleave, M. E., & Nelson, C. C. (2007). Differential regulation of clusterin and its isoforms by androgens in prostate cells. *Journal of Biological Chemistry*, *282*(4), 2278–2287. https://doi.org/10.1074/jbc.M608162200

Crowell, P. D., Fox, J. J., Hashimoto, T., Diaz, J. A., Navarro, H. I., Henry, G. H., Feldmar, B. A., Lowe, M. G., Garcia, A. J., Wu, Y. E., Sajed, D. P., Strand, D. W., & Goldstein, A. S. (2019). Expansion of Luminal Progenitor Cells in the Aging Mouse and Human Prostate. *Cell Reports*, *28*(6), 1499-1510.e6. https://doi.org/10.1016/j.celrep.2019.07.007

de Souza, N. (2017). Organoid culture. *Nature Methods*, *14*(1), 35–35. https://doi.org/10.1038/nmeth.4122

Feng, Q., & He, B. (2019). Androgen Receptor Signaling in the Development of Castration-Resistant Prostate Cancer. In *Frontiers in Oncology* (Vol. 9, p. 858). Frontiers Media S.A. https://doi.org/10.3389/fonc.2019.00858

Fink, D., Fazli, L., Aronow, B., Gleave, M. E., & Ong, C. J. (2006). Clusterin is not essential for androgen-regulated involution and regeneration of the normal mouse prostate. *The Prostate*, *66*(13), 1445–1454. https://doi.org/10.1002/pros.20461

Goto, K., Salm, S. N., Coetzee, S., Xiong, X., Burger, P. E., Shapiro, E., Lepor, H., Moscatelli, D., & Wilson, E. L. (2006). Proximal Prostatic Stem Cells Are

Programmed to Regenerate a Proximal-Distal Ductal Axis. *Stem Cells*, *24*(8), 1859–1868. https://doi.org/10.1634/stemcells.2005-0585

Huang, Y., Jiang, X., Liang, X., & Jiang, G. (2018). Molecular and cellular mechanisms of castration resistant prostate cancer. In *Oncology Letters* (Vol. 15, Issue 5, pp. 6063–6076). Spandidos Publications. https://doi.org/10.3892/ol.2018.8123

Kim, E. H., & Bullock, A. D. (2018). Surgical Management for Prostate Cancer. *Missouri Medicine*, *115*(2), 142–145. http://www.ncbi.nlm.nih.gov/pubmed/30228706

Korsten, H., Ziel-van der Made, A., Ma, X., van der Kwast, T., & Trapman, J. (2009). Accumulating progenitor cells in the luminal epithelial cell layer are candidate tumor initiating cells in a Pten knockout mouse prostate cancer model. *PLoS ONE*, *4*(5), 25–27. https://doi.org/10.1371/journal.pone.0005662

Litwin, M. S., & Tan, H. J. (2017). The diagnosis and treatment of prostate cancer: A review. In *JAMA - Journal of the American Medical Association* (Vol. 317, Issue 24, pp. 2532–2542). American Medical Association. https://doi.org/10.1001/jama.2017.7248

Matsumoto, H., Yamamoto, Y., Shiota, M., Kuruma, H., Beraldi, E., Matsuyama, H., Zoubeidi, A., & Gleave, M. (2013). Cotargeting androgen receptor and clusterin delays castrate-resistant prostate cancer progression by inhibiting adaptive stress response and AR stability. *Cancer Research*, *73*(16), 5206–5217. https://doi.org/10.1158/0008-5472.CAN-13-0359

Merriel, S. W. D., Funston, G., & Hamilton, W. (2018). Prostate Cancer in Primary Care. In *Advances in Therapy* (Vol. 35, Issue 9, pp. 1285–1294). Springer Healthcare. https://doi.org/10.1007/s12325-018-0766-1

Mirosevich, J., Bentel, J. M., Zeps, N., Redmond, S. L., D'Antuono, M. F., & Dawkins, H. J. S. (1999). Androgen receptor expression of proliferating basal and luminal cells in adult murine ventral prostate. *Journal of Endocrinology*, *162*(3), 341–350. https://doi.org/10.1677/joe.0.1620341

Moretti, R. M., Marelli, M. M., Mai, S., Cariboni, A., Scaltriti, M., Bettuzzi, S., & Limonta, P. (2007). Clusterin isoforms differentially affect growth and motility of prostate cells: Possible implications in prostate tumorigenesis. *Cancer Research*, *67*(21), 10325–10333. https://doi.org/10.1158/0008-5472.CAN-07-0516

Sala, L., Boutillon, F., Menara, G., De Goyon-Pélard, A., Leprévost, M., Codzamanian, J., Lister, N., Pencik, J., Clark, A., Cagnard, N., Bole-Feysot, C., Moriggl, R., Risbridger, G. P., Taylor, R. A., Kenner, L., Guidotti, J. E., & Goffin, V. (2017). A rare castration-resistant progenitor cell population is highly enriched in Pten-null prostate tumours. *Journal of Pathology*, *243*(1), 51–64. https://doi.org/10.1002/path.4924

Shannan, B., Seifert, M., Leskov, K., Willis, J., Boothman, D., Tilgen, W., & Reichrath, J. (2006). Challenge and promise: Roles for clusterin in pathogenesis, progression and therapy of cancer. In *Cell Death and Differentiation* (Vol. 13, Issue 1, pp. 12–19). Nature Publishing Group. https://doi.org/10.1038/sj.cdd.4401779

Shen, M. M., & Abate-Shen, C. (2010). Molecular genetics of prostate cancer: New prospects for old challenges. In *Genes and Development* (Vol. 24, Issue 18, pp. 1967–2000). Cold Spring Harbor Laboratory Press. https://doi.org/10.1101/gad.1965810

Siegel, R. L., Miller, K. D., & Jemal, A. (2020). Cancer statistics, 2020. *CA: A Cancer Journal for Clinicians*, *70*(1), 7–30. https://doi.org/10.3322/caac.21590

Song, H., Zhang, B., Watson, M. A., Humphrey, P. A., Lim, H., & Milbrandt, J. (2009). Loss of Nkx3.1 leads to the activation of discrete downstream target genes during prostate tumorigenesis. *Oncogene*, *28*(37), 3307–3319. https://doi.org/10.1038/onc.2009.181

Statz, C. M., Patterson, S. E., & Mockus, S. M. (2017). mTOR Inhibitors in Castration-Resistant Prostate Cancer: A Systematic Review. In *Targeted Oncology* (Vol. 12, Issue 1, pp. 47–59). Springer-Verlag France. https://doi.org/10.1007/s11523-016-0453-6

Steinberg, J., Oyasu, R., Lang, S., Sintich, S., Rademaker, A., Lee, C., Kozlowski, J. M., & Sensibar, J. A. (1997). Intracellular levels of SGP-2 (Clusterin) correlate with tumor grade in prostate cancer. *Clinical Cancer Research*, *3*(10), 1707–1711.

Tan, M. E., Li, J., Xu, H. E., Melcher, K., & Yong, E. L. (2015). Androgen receptor: Structure, role in prostate cancer and drug discovery. In *Acta Pharmacologica Sinica* (Vol. 36, Issue 1, pp. 3–23). Nature Publishing Group. https://doi.org/10.1038/aps.2014.18

Tsujimura, A., Koikawa, Y., Salm, S., Takao, T., Coetzee, S., Moscatelli, D., Shapiro, E., Lepor, H., Sun, T. T., & Lynette Wilson, E. (2002). Proximal location of mouse prostate epithelial stem cells: A model of prostatic homeostasis. *Journal of Cell Biology*, *157*(7), 1257–1265. https://doi.org/10.1083/jcb.200202067

Wang, X., Kruithof-De Julio, M., Economides, K. D., Walker, D., Yu, H., Halili, M. V., Hu, Y.-P., Price, S. M., Abate-Shen, C., & Shen, M. M. (n.d.). *A luminal epithelial stem cell that is a cell of origin for prostate cancer*. https://doi.org/10.1038/nature08361

Weiner, A. B., Cohen, J. E., DeLancey, J. O., Schaeffer, E. M., & Auffenberg, G. B. (2019). Surgical versus Medical Castration for Metastatic Prostate Cancer: Use and Overall Survival in a National Cohort. *Journal of Urology*. https://doi.org/10.1097/ju.0000000000000684

Welch, H. G., & Albertson, P. C. (2009). Prostate cancer diagnosis and treatment after the introduction of prostate-specific antigen screening: 1986-2005. *Journal of the National Cancer Institute*, *101*(9), 1325–1329. https://doi.org/10.1093/jnci/djp278

Wilson, M. R., & Zoubeidi, A. (2017). Clusterin as a therapeutic target. *Expert Opinion on Therapeutic Targets*, *21*(2), 201–213. https://doi.org/10.1080/14728222.2017.1267142

Zoubeidi, A., Chi, K., & Gleave, M. (2010). Targeting the cytoprotective chaperone, clusterin, for treatment of advanced cancer. *Clinical Cancer Research*, *16*(4), 1088–1093. https://doi.org/10.1158/1078-0432.CCR-09-2917